ARMA 15-0394

Induced Microseismic Monitoring in Salt Caverns

Hosseini, Z., Collins, D., Shumila, V., Trifu, C.I.
ESG Solutions, Kingston, Ontario, Canada
Pinnock, I.
ESG Solutions, Perth, Australia

This paper was prepared for presentation at the 49th US Rock Mechanics / Geomechanics Symposium held in San Francisco, CA, USA, 28 June-1 July 2015.

ABSTRACT: In recent years, salt cavern failures and sinkholes associated with brine wells in solution mining have created concerns and initiated more restrict regulations and guidelines for solution mining operations. One of the monitoring tools for cavern stability relates to tracking passive microseismic activity during brine well operation. Any gradual or sudden rockmass failure is often associated with pre-failure microfracturing activity in the rockmass which leads to microseismic activity. A suitably designed microseismic system with sufficient sensitivity can capture the pre-failure activity days or months before the failure and along with other instrumentation and geotechnical analysis can provide critical information that can be used to help identify and possibly reduce the risk of catastrophic rockmass failure. This paper presents two cases of induced microseismic monitoring in soft rock media and of salt caverns created by solution mining. An example of a microseismic system installation and calibration in a salt cavern is demonstrated, and the results of advanced analysis from a second salt cavern monitoring are briefly investigated

1. INTRODUCTION

Microseismic systems were initially developed for applications in underground hard rock mining due to increased microseismic activity initiated by higher mining depths and therefore higher stress levels. The increased seismic activity and violent rockbursts causing damage and fatalities led to more rapid development of this technology. The main purpose of early microseismic systems was to enhance safety in seismic active areas of the mine. The early systems were only able to provide approximate information on location and magnitude of seismic events.

Today, however, the high-end technology is capable of recording full waveforms on a continuous basis that can further be processed through advanced seismology codes and powerful computers for additional understanding of the rockmass behavior. The systematic mechanism and source parameter analysis of seismic events can now be reliably used as a geotechnical tool to assess strain/stress changes in the monitored volume.

This paper aims to review the potential applications of monitoring induced microseismic activity in salt caverns.

Over the last few years, a number of salt caverns collapsed in New Mexico and Louisiana. Some of these collapses were associated with elevated microseismic activity before cavern failure.

Following these failures, a Carlsbad brine well operation installed a seismic system around one of its major salt caverns for real time monitoring of induced microseismic activity. The system design, installation, calibration, and some of the data recorded to date will be reviewed in this paper.

In the next section of this paper, the results of advanced seismic analysis of another salt cavern for the purpose of a controlled collapse in Romania will be briefly discussed. In this case, systematic analysis of seismic data, clusters, source mechanisms and deformations determine the process of gradual cavern fracturing and failure.

2. SALT CAVERN

In solution mining, fresh water is injected into the salt formation to create a highly saturated brine. The brine is then extracted through the brine well, and used for drilling operations in the oil and gas industry. This process over time creates a cavern underground in the salt.

A salt cavern is subject to a risk of collapse, and a few factors contributing to collapse are the shallow depth of the salt layer, the type of the well, the method of extraction, the strength of the overlaying material, and the volume of salt extracted (cavern volume). One of the main factors contributing to salt cavern stability is maintaining a cavern diameter/depth ratio of 2/3, otherwise the cavern may fail resulting in a gradual ground subsidence or major collapse. There might be early warning signs associated with the collapse, such as an increased rate of abnormal seismic activity within days or months before collapse. In 2008, failure of two brine well caverns in New Mexico resulted in massive sinkholes causing significant damage, and creating public panic and evacuations [1].

In August 2012, another sinkhole was discovered in Louisiana. This sinkhole was caused by the Bayou Corne Brine well, operated by Texas Brine Company. Some early signs including elevated seismic activity were reported by residents as early as June.

In New Mexico, Jim's Water Brine well collapsed on July 16, 2008. The initial sinkhole was about 40 ft wide and by April 2009 it grew to 400 ft across and 120 ft deep (Fig 1). The sinkhole was reported to continue growing after that.

Fig. 1: Jim's Water Brine well, on Aug. 26, 2008. Photo courtesy of the National Cave and Karst Research Institute

A report by Oil Conservation Division (OCD) [1] indicates that a seismograph located about 8 miles away from Jim's Water Brine well, had recorded a series of seismic events about 6 hours before the surface collapse started.

The second well, Loco Hills brine well, collapsed in November 2008. The well created a similar sinkhole over time as Jim's Water Brine well. In this case, the seismograph was about 14 miles away and didn't record any seismic activity before the collapse.

At the end of their study, OCD issued a set of recommendations for solution mining procedures, brine well requirements, real time monitoring and implementing early warning systems for the remaining brine well operations in the region.

In this paper, results from a Carlsbad brine well microseismic monitoring system are presented. The goal of the system was to monitor any abnormal seismic activity around the brine well and the salt cavern in real time.

3. MICROSEISMIC SYSTEM

3.1. Seismic System Design

A 24-channel microseismic system was custom designed and installed by ESG Solutions for this site which is referred to in this paper as the Carlsbad salt cavern. Four boreholes were selected for final installation of sensor strings. Three out of the four boreholes have a depth of 400 ft., and one with a depth of 700 ft.

At the design stage, the number and type of microseismic sensors were carefully assessed and determined based on the rock type, geological structures, rockmass characteristics, and the size of the monitored volume. It is also important to consider the objectives of the seismic monitoring at the design stage; the accuracy and sensitivity of the system and system's capability to collect data suitable for advanced analysis or other parameters such as evaluating acceleration or peak particle velocity all have to be taken into account at this initial phase.

The recommended array design for the Carlsbad salt cavern provided a location accuracy of 10-40 ft., with a minimum Moment Magnitude (Mw) of -2.3, and the ability to identify fracture sizes of around 5-6 ft (Fig. 2).

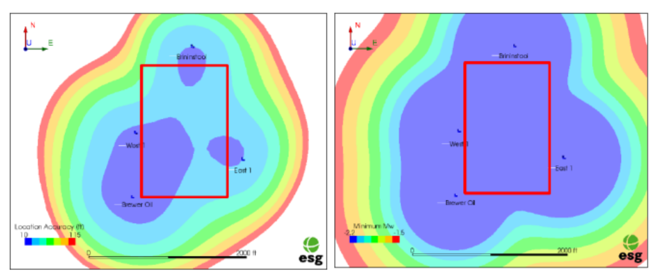

Fig. 2 Location accuracy (left) and minimum detectability (right) analysis at elevation of 2678 ft. which is the top of the salt layer. The red rectangle identifies the volume of interest around the cavern

The type of rock that seismic sensors are installed in, can significantly affect the signal content and quality. In a hard rock (high density and elasticity modulus) that contains little jointing and fracturing, both high and low frequency seismic waveforms can travel further while maintaining their frequency content. In this, case both accelerometers and geophones can be used to record a wider range of magnitude events as low as -3 Mw. In soft rock material, however, such as salt, potash, and coal, the high frequency content of the waveform is attenuated more rapidly with distance, [2], and therefore, slightly lower frequency response geophones are recommended.

In a media with different rock types, sensors should be installed in a volume with less fractures and higher elastic modulus and density. The strata in the Carlsbad site is made up of alluvium, anhydrite, and halite (salt) amongst other minerals. Table **1** shows the initial and enhanced elevation as well as wave velocity in the layers at this site based on sonic log data and further velocity calibration analysis by ESG.

Table 1. Boundary elevation and P-wave velocity based on sonic log data. S-wave velocity is assumed to be Vp/1.73

Rock Type	Elevation (positive up)
Alluvium	3134-2963ft
Anhydrite/Limestone/Gypsum	2963-2678ft
Salt	<2678ft

Layer	Elevation Range (ft)	IWMS1 (ft/s)	IWMS2 (ft/s)	IWMS3 (ft/s)	IWMS4 (ft/s)	Avg Velocity Vp (ft/s)
1	3123 - 3032	N/A	10952	9404	N/A	10178
2	3032 - 2887	N/A	7324	6937	N/A	7131
3	2887 - 2720	11945	13467	12887	N/A	12766
4	2720 - 2523	N/A	N/A	N/A	12839	12839
5	< 2523	N/A	N/A	N/A	14924	14924

In the case under study, the alluvium layer, with a thickness of 170 ft starting from the surface, is the least competent media compare to the underlying layers. To avoid installing sensors inside the alluvium layer, the first sensor was recommended to be installed at a minimum depth of 200 ft below surface (Fig. 3).

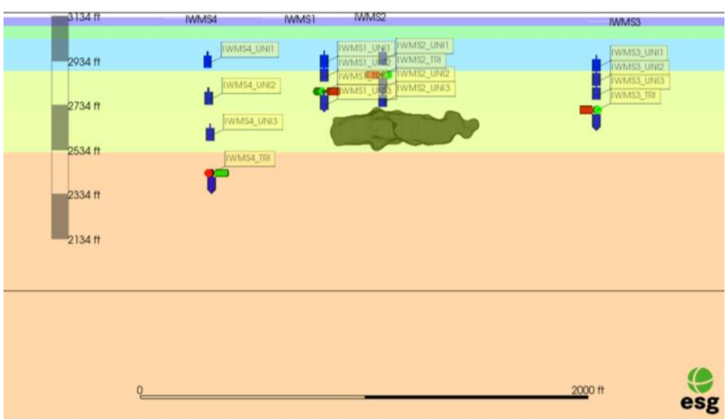

Fig. 3: Section view of the cavern and seismic sensors inside borehole

3.2. *Seismic System Install and Calibration*

After the design was approved, a 24-ch system consisting of 12 uniaxial and four triaxial 15Hz geophones was installed inside the four boreholes selected.

The system was installed in October 2013. One junction box including one 6-ch Paladin data logger, GPS antenna for time synchronization of all stations, radio antennas, and solar panels was installed close to the collar of each of the four boreholes (Fig. 4).

Fig. 4: Lowering sensor arrays in the borehole (left); and setting up the Paladin junction box at one station (right)

3D Velocity Model

The sonic log data from each of the four boreholes were used to develop the initial horizontal layered velocity model for five layers, Fig. 5. A sixth layer near surface was later added using advanced algorithms to account for slower surface layers that were not accurately accounted for in the sonic log data.

In the next step, advanced analysis and calibration drop test data were used to further enhance the velocity model. To calibrate the system, 10 drop tests were completed on site using a 3000 lb. block with a drop height of 10 ft. at different coordinates around the site. The sensors' orientations were then determined using drop test and optimized velocity model data. All boreholes are vertical, except for the 700 ft hole where the deviation log was used to calculate the sensor locations inside the borehole.

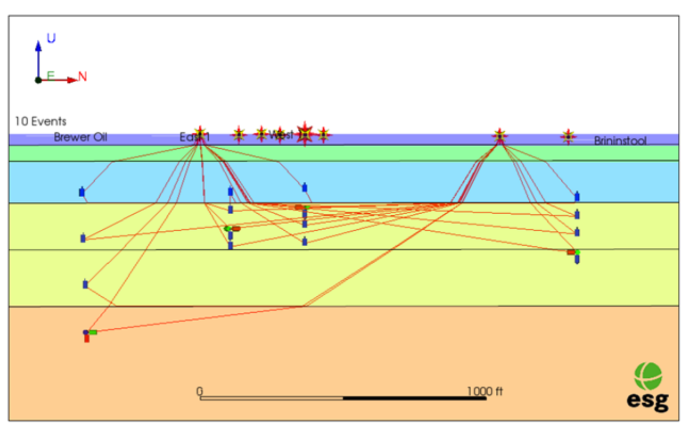

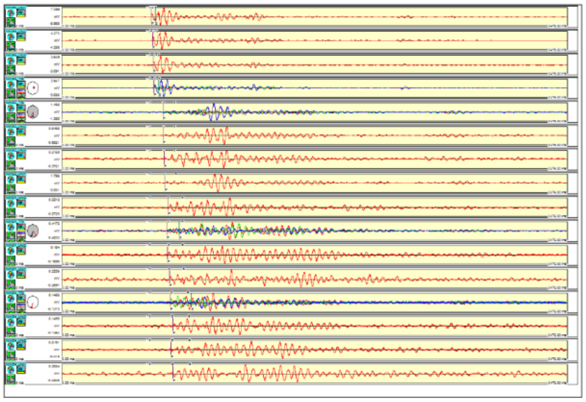

Fig. 5: Layered velocity model showing different ray paths of two drop tests (top) waveforms created by a drop test and recorded on all sensors (bottom)

With further optimization, all sensors were tested and passed as operational with low noise levels typical for 15Hz geophones. The sensors closer to surface show slightly higher noise levels (surface noise) which is not significant enough to affect data quality adversely.

The optimization analysis also confirmed that all triaxial sensors have a high linearity number (between 64-86%) which represents good coupling with the rockmass and good signal quality.

In the next step a 3D velocity model was developed using advanced algorithms [3] to take into account the shape of the cavern and to further increase the location accuracy. Table 2 shows the modified P-wave velocities for each layer. A P-wave velocity of 5,300 ft/s was assigned to the brine filled cavern.

A 3D velocity model accounts for more realistic ray paths from the seismic source to the sensor as it travels through different shaped geology and material such as fluids.

As shown in Fig. 6, the P-wave velocity isolines are significantly perturbed by the presence of the brine filled cavern. Outside of the cavern zone, the isolines vary due to the presence of the layered velocity model.

Table 2: Updated velocity model upon completion of drop tests and including the cavern outline into the 3D model

Layer#	Elevation[1] (ft)	V_P velocity estimates (ft/sec)		
		Original[2]	New	Difference
1	3130	5272.5	5591.2	318.7
2	3090	10226.4	9013.4	-1213
3	3032	7173.4	8612.2	1438.8
4	2887	12718.2	12731.1	12.9
5	2720	12789.9	12790.1	0.2
6	2523	14930.5	14973.3	42.8

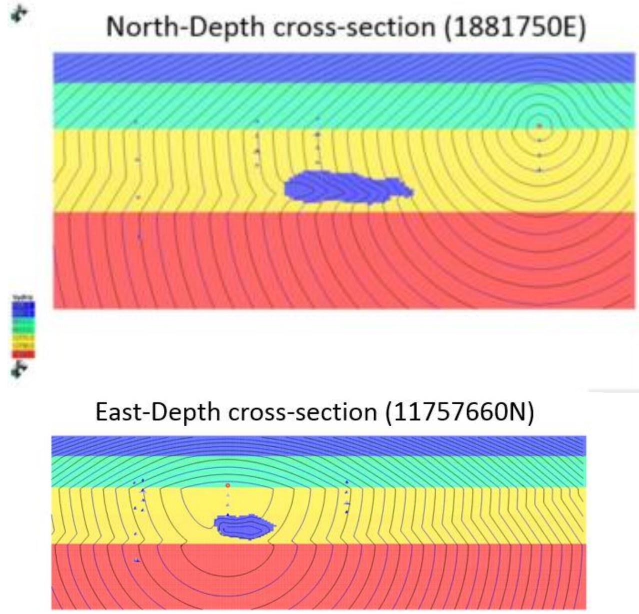

Fig. 6: P-wave travel time isolines for a seismic source (red dot). Changes are seen in the isolines as they pass through different layers and the salt cavern (blue mass).

Furthermore Fig. 7 shows ray-tracing between a hypothetical seismic source (green dot) near the cavern edge to a seismic sensor (red dot) and how the new 3D velocity model produces a realistic raypath (black line) around the cavern void.

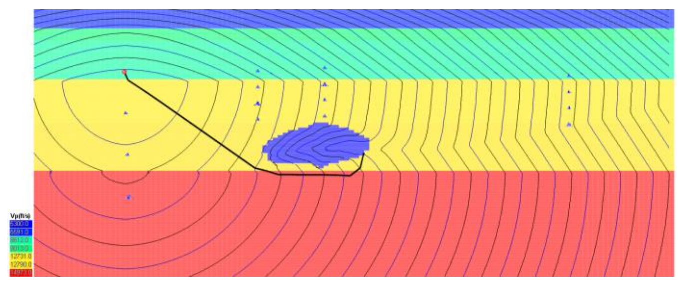

Fig. 7: Ray tracing of a hypothetical source near the cavern as it reaches one of the sensors (red dot). The remaining sensors are shown as blue dots.

The software-created examples above demonstrated that the full 3D velocity model behaves as expected and can be used in the advanced source location algorithm as well as the advanced analysis methods such as source mechanism determination (seismic moment tensor). This advanced 3D velocity model is currently used for daily seismic event monitoring of the cavern.

The seismic system has been operational since the install and optimization to monitor any unusual seismic activity around the cavern. The sensors trigger on surface noise and seismic events. Since there is no active operation at the site, it is expected that the level of induced seismicity should be minimal (Fig. 8). The majority of triggers have a magnitude range of -0.9 to +0.2 Mw.

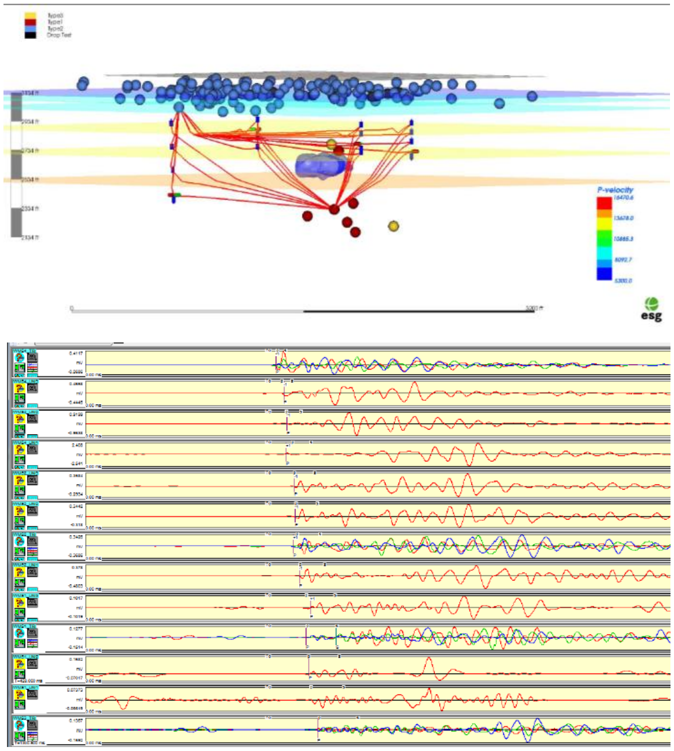

Fig. 8: Data recorded at the Carlsbad salt cavern over an 8-month period and the path of fastest P-wave from a seismic event to all sensors determined by the 3D velocity model (top). An example of an event waveform recorded by all sensors (bottom).

Most triggers are recorded between the hours of 8:00- 18:00 which indicates daily activities on surface and nearby roads and building which triggers the sensors (Fig. 9).

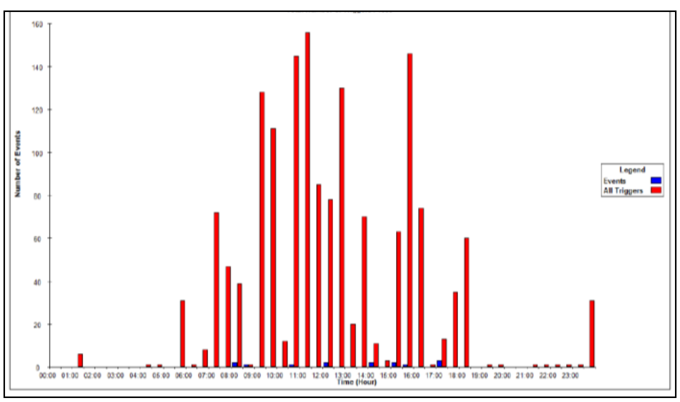

Fig. 9: Time of day plot showing real events in blue and all triggers in red.

In general, events can be categorized into three types depending on P-wave and S-wave arrival clarity, frequency content and length of signal recorded:

- Type 1: Triggers with a dominant frequency content of 50Hz, and signal length of 300-500 ms. These triggers locate at depth with higher confidence in location accuracy and can be indicative of real seismic events which relates to fracturing in the competent rockmass, Fig. 10.
- Type 2: Triggers with a dominant Frequency content of 20-30Hz, and signal length of 300-800 ms. These events are most likely surface noise which include the majority of triggered events with lower confidence in location accuracy.
- Type 3: Triggers with a dominant frequency content on triaxial sensors of 22-33Hz, and signal length more than 1000 ms. with emerging signal. These events are indicative of a long duration seismic event occurring underground

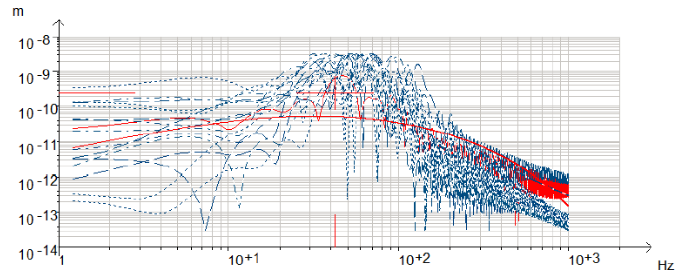

Fig. 10: Superimposed P-wave displacement spectra for event type 1

The event types can be determined through manual processing; however, the event identification in semi-real time can be improved in two ways:

- Hardware: By installing an additional low-frequency triaxial sensor on surface
- Software: By developing an advanced software algorithm that can classify trigger types based on spectral frequency content and signal duration of waveforms

3.3. Advanced Seismic Analysis

Before performing advanced analysis, the data set consisting of over 12,000 triggers was re-processed to eliminate all noise triggers totaling about 11,800 and verify the classification of the remaining events into types 1 to 3. Fig. 11 shows the reprocessed data using the optimized 3D velocity model.

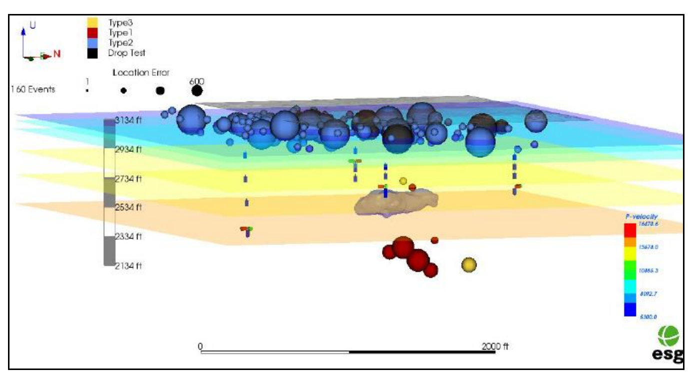

Fig. 11: Re-processed event distribution

Fig. 12 shows that the majority of events are within a magnitude range of -2 to 0.0 Mw, with a large portion of smaller magnitude numbers.

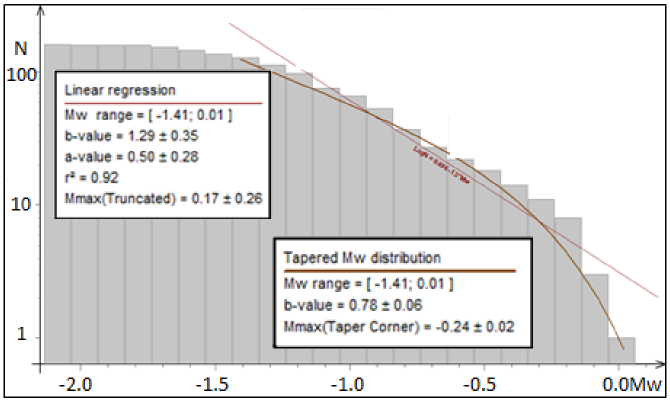

Fig. 12: Event- magnitude distribution of all seismic data at the Carlsbad salt cavern site.

There has not been an elevated seismic activity at the site since the installation of the seismic system; however, a total of eight seismic events were recorded within the monitoring zone and selected for advanced analysis in late 2014 (see Fig. 13). The events occurred in the months of February, May, June and August of 2014.

The bottom left plot in Fig. 13 shows the 3D strain axes for these events. The red arrows are indicative of inward strain and the blue axes show outward strain.

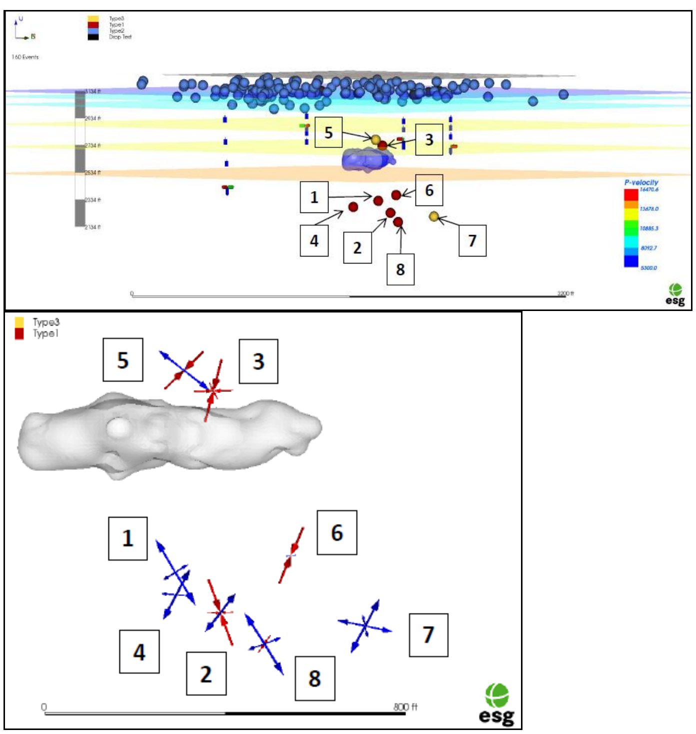

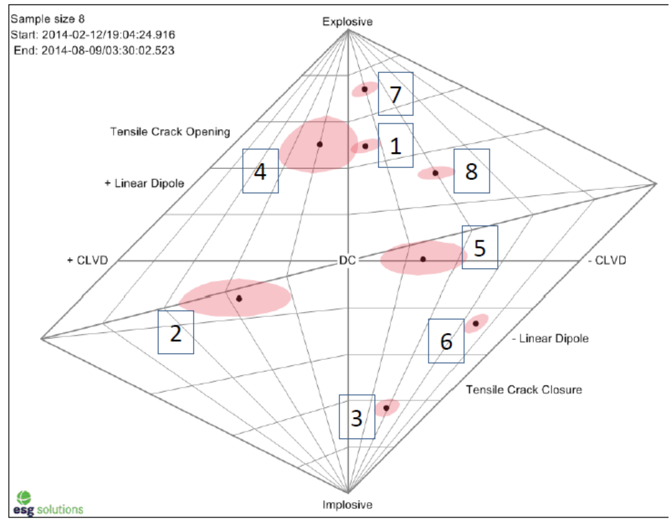

Fig. 13: Selected events for advanced analysis (top); inward/ outward strain axes in red and blue respectively showing the mechanism results (middle); Source type diagram showing mechanism types (bottom).

The bottom plot in Fig. 13 shows the mechanism type diagram for these events. The elliptical shades indicate the confidence level for each mechanism solution. Events 1, 4, 7 and 8 show a dominant opening mechanism, while events 3 and 6 have a dominant closing mechanism, and events 2 and 5 are dominantly shear slip events.

Identification of the source mechanisms provides valuable information as to the modes of strata failure. The seismic information combined with data measured by other instrumentation that may have been installed at the site such as water pressure, tilt meters, or other displacement measurement units, provides an important way to assess cavern stability.

In summary, the seismic system at Carlsbad has been designed and optimized to continuously monitor background and abnormal activity. The site has put priority on maintaining the seismic system and consistently processing all seismic triggers. To date there has been no major seismic activity that can be indicative of concerns with regards to the stability of the cavern.

Continuously maintaining a clean record of seismic activity and analysis of each major event or cluster allows for early assessment of any changes in rockmass behavior at early stages.

In the next steps it is recommended to correlate seismic activity with site activities as well as data measured from other instrumentation mentioned above.

4. SALT CAVERN MONITORING, ROMANIA

A second case of salt dome monitoring relates to a controlled collapse of the Ocnele Mari salt caverns in southern Romania. Production started in 1950s, and a major collapse occurred in 1991 in field II of the four fields following an extraction of 13.5 M tons of salt. Two other failures occurred in 2001 and 2004 which prompted a need for action and change of strategy [4].

To eliminate the risk of a sudden failure of the main salt cavern near a populated area, a controlled collapse was implemented. The strategy included the extraction of brine and replacing it with fresh water simultaneously to avoid turbulence in the overall hydraulic pressure status and to let the roof collapse under its own weight in a more controlled manner.

A microseismic system was installed over an area of 1 km^2 in advance to safely monitor the process and assess the rockmass response. Quantitative analysis of seismic events was completed to determine failure mechanisms and trends throughout the process.

The system, built by ESG Solutions, included six Paladin data loggers and 36 uniaxial 15Hz geophones installed in 12 boreholes from surface with depths ranging from 160-360 m. During a nine month monitoring period, 2,392 microseismic events with moment magnitudes of -2.6 to 0.2 Mw were recorded [5].

The analysis of the seismic data showed that the collapse initiated as a linear fracture pattern for the first three months where fracturing and fragmentation occurred in the cavern roof. A shear dominated fracturing occurred after that which expanded into fracturing throughout the entire monitoring volume up to a month following the roof collapse.

The data were also reprocessed using a collapsing technique [6] to identify and study major clusters of seismicity (see Fig. 14). The clusters showed that the majority of activity was associated with the roof failure of the main cavern and some activity associated with the sides and the floor of the cave. Some other smaller and less active clusters seemed to be associated with the collapse of the surrounding smaller size caverns.

4.1. Source Mechanism analysis

Source mechanism analysis was performed on the dataset resulting in 912 with acceptable solutions. Mechanism results were excluded if the condition number was > 100 (ill-conditioned matrix) or $r^2 < 0.5$ (poor fit of model to data). Since the area of monitoring was subject to three major previous collapses and therefore pre-existing fractures and damage to the salt dome, the seismic records were expected to yield a range of failure for the various volumes that were monitored.

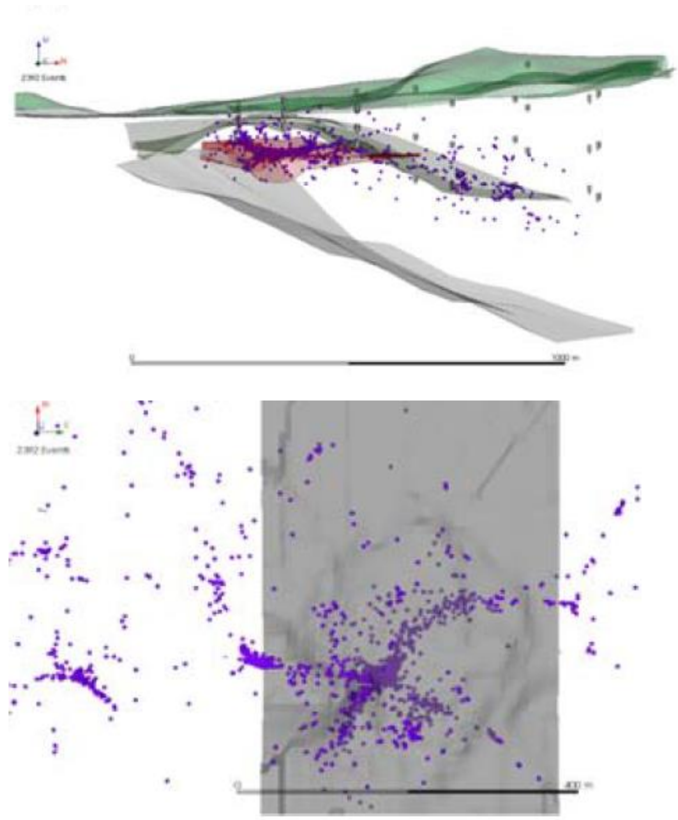

Fig. 14: Relative seismic event location in section (top) and plan views (bottom).

Fig. 15 shows the source mechanism results. The gray rectangle shows the area of the major cavern that previously collapsed in 2011. The spatial scattered pattern, around the cavern indicates the varying local stress distribution and continuous failure along existing fractures. At the same time, the semi-circular and radial orientation of Tensile and Pressure axes around the sinkhole are identifiable. The analysis of double couple (DC) components show that the largest pure shear (DC) component is associated with events around the cavern roof with normal to strike-slip failure behaviors, as expected.

Only a small percentage of events exhibited an implosional failure type which seems to be caused by the impact of fallen material from the roof (under gravity) to the floor of the cavern. A significant 30% of events showed explosional behavior which is associated with peeling off of the material from the roof and their collapse under gravitational loads.

4.2. Seismic deformation field

Moment tensor solutions were further analyzed to determine the strain rate tensor components in horizontal and vertical directions. The higher strain values seem to be associated with the pre-existing fractures in the roof and floor of the cavern, while the highest horizontal strain is most prominent in the collapsed zones, Fig 16

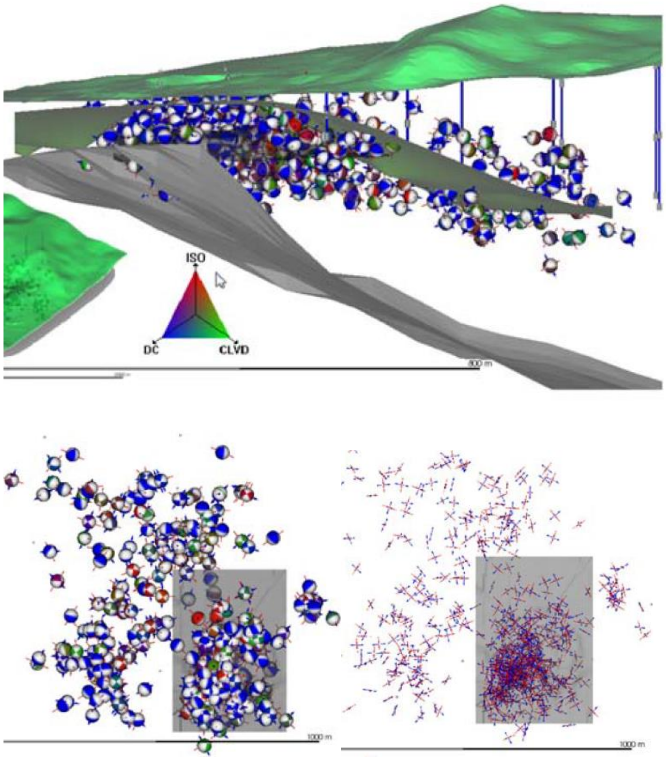

Fig. 15: Event mechanism solutions in section (top) and plan view (bottom).

This study was the first of its type to monitor induced microseismicity associated with a controlled salt cavern collapse and advanced analysis of seismic events associated with the cavern failure process.

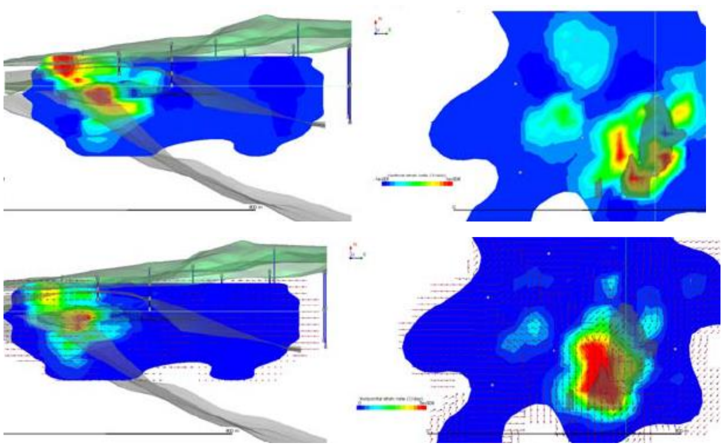

Fig 16: Vertical strain rates (top) and horizontal strain rates (bottom)

5. CONCLUSION

The microseismic monitoring system at the Carlsbad salt cavern site has operated since October 2013. The system was designed based on the site geology and monitoring requirements to ensure real time monitoring and alerting with a reasonable seismic location accuracy and magnitude sensitivity. The 24-channel system is installed inside four deep boreholes around the salt cavern, and seismic triggers are transferred to the engineering office via radio links.

A 3D velocity model was developed for the array taking into account the different rock layers and velocity models as well as the 3D shape of the cavern to increase event location accuracy.

There has been no major seismic activity within the monitored volume to suggest cavern instability. However a few seismic events were located mostly at depth and around the cavern which indicates occasional seismic activity and minor stress redistribution changes around the brine operation zone. Analysis of these events indicate that there is a mixture of opening, closing and shear mechanisms. A closer study that takes into account the daily operation activities at the site plus the data from other measuring instruments on site can provide more insight into the causes and possible consequences for the cavern. Such routine analysis of all data is critical in detecting any abnormal ground activity that could result in a catastrophic failure. Such analysis may help prevent or minimize the impact of a rockmass failure.

In the second part of this paper, another case of salt cavern monitoring was reviewed. In this case, a controlled collapse of the salt cavern created more than 2300 seismic events over a nine month period. Capturing this number of microseismic events was made possible through a suitable system design with proper sensor types and numbers that considered the soft rock nature of the monitored volume.

Although the primary objective of the seismic system was the safety of crew and equipment on a daily basis, a set of advanced analyses including relocating data using the collapsing technique, phased source mechanism analysis on select data of higher quality, and seismic deformation field analysis revealed fracture development progress that explains how the cavern roof collapsed in response to the controlled collapse strategy.

The analysis showed an initial fracture network development for the first few months with a dominant linear fracturing pattern, followed by shear failures associated with the roof collapse. Seismicity associated with further fracturing of the strata surrounding the cavern continued for another month beyond the major collapse.

Solution mining technology has advanced over the years. Advanced and real time monitoring tools are now a major part of operations for many brine well sites. Maintaining a clean record of all field data and routinely study data from each instrument is critical. In addition, analysis of combined data to correlate rockmass reactions and movements to brine extraction is essential.

Most rockmass failures start with a few signals and early indications of failure process initiation. These early indications can be captured in a timely manner with the right monitoring tools such as microseismic monitoring, ground water pressure changes, and measurement of vertical and horizontal displacement, and other techniques.

The focus of this paper was mainly on the feasibility of passive seismic monitoring in salt formations with solution mining operations. However, for future analysis, it is recommended to incorporate daily mining activities, site geotechnical information as well as data from other instruments into the advanced seismic analysis to obtain a more precise rockmass response to solution mining operations in near-real time. Such analysis can be critical in optimizing salt cavern stability and reducing the risk of catastrophic failures.

REFERENCES

1. Oil Conservation Division Environmental Bureau, 2009 Brine Well Collapse Evaluation Report.
2. Wu, X., Liu, C., Hosseini, Z., 2012. Applications of Microseismic Monitoring in China's Underground Coal Mines. *In Proceedings of 31st International Conference on Ground Control in Mining*
3. Collins DS, Toya, Y, Pinnock I, Shumila V, Hosseini Z, 2014, '3D velocity model with complex geology and voids for microseismic location and mechanism', *In Proceedings of the 7th International Conference on Deep and High Stress Mining, September, Sudbury*, ACG, pp 681-688
4. Zamfirescu, F., Mocuta, M., Dima, R., Constantinescu, T., and Nita, C., 2007. A technical solution for the collapse fragmentation of the field II cavern – Ocnele Mari, Romania, *In Proceedings of Solution Mining Research Institute Spring meeting, 28 April – 2 May, 2007b*, Basel, Switzerland, 8 pp.
5. Trifu, C., Shumila, V., 2010. Microseismic monitoring of a controlled collapse in filed II at Ocnele Mari, Romania. J. *Pure Applied Geophysics*. 167, Issue 1-2, pp 27-42
6. Jones, R.H., Steward, R.C. 1977. A method for determining significant structures in a cloud of earthquakes. *J. Geophysical. Res.* 102, 8245-8254